




# Sde2 is an intron-specific pre-mRNA splicing regulator activated by ubiquitin-like processing

Poonam Thakran<sup>1,†</sup> , Prashant Arun Pandit<sup>1,†</sup>, Sumanjit Datta<sup>1</sup> , Kiran Kumar Kolathur<sup>1</sup>, Jeffrey A Pleiss<sup>2</sup> & Shravan Kumar Mishra<sup>1,\*</sup> 

## Abstract

The expression of intron-containing genes in eukaryotes requires generation of protein-coding messenger RNAs (mRNAs) via RNA splicing, whereby the spliceosome removes non-coding introns from pre-mRNAs and joins exons. Spliceosomes must ensure accurate removal of highly diverse introns. We show that Sde2 is a ubiquitin-fold-containing splicing regulator that supports splicing of selected pre-mRNAs in an intron-specific manner in *Schizosaccharomyces pombe*. Both fission yeast and human Sde2 are translated as inactive precursor proteins harbouring the ubiquitin-fold domain linked through an invariant GGKGG motif to a C-terminal domain (referred to as Sde2-C). Precursor processing after the first di-glycine motif by the ubiquitin-specific proteases Ubp5 and Ubp15 generates a short-lived activated Sde2-C fragment with an N-terminal lysine residue, which subsequently gets incorporated into spliceosomes. Absence of Sde2 or defects in Sde2 activation both result in inefficient excision of selected introns from a subset of pre-mRNAs. Sde2 facilitates spliceosomal association of Cactin/Cay1, with a functional link between Sde2 and Cactin further supported by genetic interactions and pre-mRNA splicing assays. These findings suggest that ubiquitin-like processing of Sde2 into a short-lived activated form may function as a checkpoint to ensure proper splicing of certain pre-mRNAs in fission yeast.

**Keywords** deubiquitinating enzymes; intron-specific pre-mRNA splicing;

N-end rule pathway; telomeric silencing; ubiquitin-like processing

**Subject Categories** DNA Replication, Repair & Recombination; Post-translational Modifications, Proteolysis & Proteomics; RNA Biology

**DOI** 10.15252/embj.201796751 | Received 16 February 2017 | Revised 11 August 2017 | Accepted 16 August 2017 | Published online 25 September 2017

**The EMBO Journal (2018) 37: 89–101**

## Introduction

Protein-coding genes in eukaryotes are often interrupted by non-coding introns. Following their transcription into precursor messenger RNAs (pre-mRNAs), the splicing process removes the introns

and joins the exons to generate translatable mRNAs. The pre-mRNAs can also undergo alternative RNA splicing to generate more than one protein-coding mRNAs from a gene. The majority of human genes have introns and undergo constitutive as well as alternative RNA splicing (Ast, 2004; Kim *et al*, 2006). The spliceosome is a large ribonucleoprotein (RNP) complex that assembles with five small-nuclear RNAs (snRNAs) and nearly two hundred proteins to perform pre-mRNA splicing. The snRNP complexes form the spliceosomal core, while RNA-binding proteins, RNP modifying enzymes (ATPases, helicases) and modifications of splicing factors (phosphorylation, methylation) regulate activity of this complex (Wahl *et al*, 2009).

Ubiquitin and ubiquitin-like proteins (collectively referred to as UBLs) share the ubiquitin-fold and act as key regulators of a variety of cellular processes including protein homeostasis, signalling, trafficking and DNA transactions (Welchman *et al*, 2005; Hochstrasser, 2009; van der Veen & Ploegh, 2012). The canonical ubiquitin is covalently conjugated to proteins by a set of enzymes in a process termed ubiquitination. Ubiquitin itself is not encoded as a single polypeptide, but rather is translated as a precursor, fused either to ribosomal protein genes, or with multiple ubiquitin moieties in tandem (Finley *et al*, 1989; Hochstrasser, 2009; Kimura & Tanaka, 2010). These precursors are processed by ubiquitin-specific hydrolases (also referred to as deubiquitinating enzymes or DUBs) immediately after di-glycine (GG) motifs to generate functional ubiquitin (Turcu *et al*, 2009).

Whereas several UBLs follow ubiquitin's mode of processing and conjugation by employing respective UBL-specific enzymes, Hub1/UBL5 lacks the di-glycine motif, and acts through a non-covalent process. Hub1 binds to the HIND domain-containing splicing factors Snu66 and/or Prp38 and functions in pre-mRNA splicing by promoting the usage of non-canonical 5' splice sites in introns. Hub1 thereby promotes alternative splicing of the *SRC1* pre-mRNA in *Saccharomyces cerevisiae* (Mishra *et al*, 2011). Specific roles of Hub1 in pre-mRNA splicing have also been reported in both *Schizosaccharomyces pombe* and mammalian cells (Wilkinson *et al*, 2004; Mishra *et al*, 2011; Ammon *et al*, 2014). Whereas *HUB1* is a non-essential gene in *S. cerevisiae*, its orthologs in *S. pombe* and mammalian cells are essential for viability, perhaps because of the increased prevalence of introns and alternative splicing in *S. pombe* and humans.

1 Max Planck – DST Partner Group, Department of Biological Sciences, Centre for Protein Science Design and Engineering, Indian Institute of Science Education and Research (IISER) Mohali, Mohali, Punjab, India

2 Department of Molecular Biology and Genetics, Cornell University, Ithaca, NY, USA

\*Corresponding author. Tel: +91 856 694 8924; E-mail: skmishra@iisermohali.ac.in, mishra.iiserm@gmail.com

<sup>†</sup>These authors contributed equally to this work

The process of pre-mRNA splicing has been linked to heterochromatin formation at the centromeres and telomeres in *S. pombe* (Bayne *et al*, 2008; Huang & Zhu, 2014; Kallgren *et al*, 2014; Wang *et al*, 2014). Earlier splicing factors were thought to provide a platform for the generation of small interfering siRNAs in the RNAi pathway of heterochromatin formation, since their mutants were defective in heterochromatin formation, but appeared normal in pre-mRNA splicing (Bayne *et al*, 2008). Recent reports however connect the heterochromatin defects observed in splicing factor mutants with reduced splicing of mRNAs encoding *bona fide* components of the heterochromatin pathway (Bayne *et al*, 2014; Kallgren *et al*, 2014; Wang *et al*, 2014). *Schizosaccharomyces pombe* lacking the *sde2* gene, named for silencing defective, showed defective telomeric silencing (Sugioka-Sugiyama & Sugiyama, 2011). Strains lacking *sde2* also showed defects in centromeric silencing and defects in splicing of cytoskeleton constituents and centromeric outer repeat transcripts (Bayne *et al*, 2014). The human ortholog of Sde2, C1orf55, was present in spliceosomal preparations (Bessonov *et al*, 2008), and recently, the *S. pombe* protein was also shown to associate with splicing factors (Bayne *et al*, 2014; Chen *et al*, 2014).

In this study, we report that *sde2* genetically interacts with *hub1* in *S. pombe*. The Sde2 protein has a ubiquitin-fold at its N-terminus, which must be cleaved by the ubiquitin-specific proteases (USPs) Ubp5 and Ubp15. After cleavage, the C-terminal domain of Sde2, which starts with a lysine, gets incorporated into the spliceosome. Loss of Sde2 results in inefficient removal of selected introns from a subset of genes having functions in telomeric silencing, DNA replication and transcription. Furthermore, the N-end rule pathway of proteasomal degradation controls the level of Sde2 protein in the cell. The intron-specific pre-mRNA splicing activity of the ubiquitin-fold-containing Sde2 protein becomes critical for chromatin silencing and genomic stability in *S. pombe*.

## Results

### Sde2 is processed like ubiquitin precursors

We have previously reported the role of the UBL Hub1 in alternative RNA splicing through usage of non-canonical 5' splice sites in the budding yeast *S. cerevisiae* (Mishra *et al*, 2011). Orthologs of Hub1 in *S. pombe* and humans are essential for viability and play specific roles in pre-mRNA splicing (Mishra *et al*, 2011; Ammon *et al*, 2014). To identify spliceosomal regulators in an intron prevalent organism, we screened for genetic interactors of *hub1* by combining *S. pombe hub1-1* mutant (Yashiroda & Tanaka, 2004) with the haploid deletion library of non-essential genes (Kim *et al*, 2010). As expected from Hub1's role in pre-mRNA splicing, deletion mutants of multiple splicing factors were synthetically sick with *hub1-1* (Fig EV1A). Among them, the deletion of *sde2* gene was also synthetically sick with *hub1-1*. We confirmed this interaction by generating double mutants of *hub1-1* with  $\Delta sde2$  independently (Fig EV1B). As reported previously in high-throughput studies (Kennedy *et al*, 2008; Zhang *et al*, 2013), the  $\Delta sde2$  strain grew slowly under standard conditions, and the growth defect was more pronounced at elevated temperatures and under genotoxic stress conditions (hydroxyurea, valproic acid, sodium butyrate, cadmium) (Appendix Fig S1A).

Putative orthologs of Sde2 exist in organisms from yeast to humans (Fig EV1C). However, in the Fungi subphylum Saccharomycotina, an Sde2-like protein is observed in *Debaryomyces*, but is absent in *S. cerevisiae*, *Candida albicans* and *Pichia pastoris*. The protein structure prediction program i-TASSER (Yang *et al*, 2015) predicted the presence of a ubiquitin-fold at the N-terminus and a C-terminal helical domain in Sde2 (henceforth referred to as Sde2<sub>UBL</sub> and Sde2-C, respectively). An invariant signature motif, GGKGG, separates the moderately conserved Sde2<sub>UBL</sub> and Sde2-C (Figs 1A and EV1C). This motif flanks Sde2<sub>UBL</sub> and resembles the di-glycine (GG) motif typical of UBL precursors processed by the UBL-specific proteases.

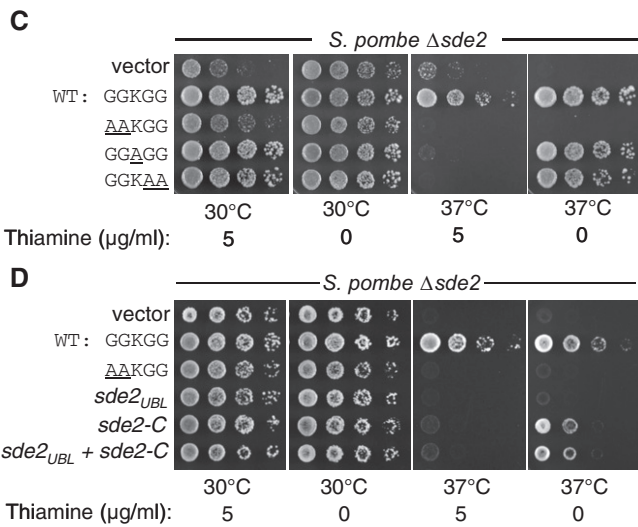
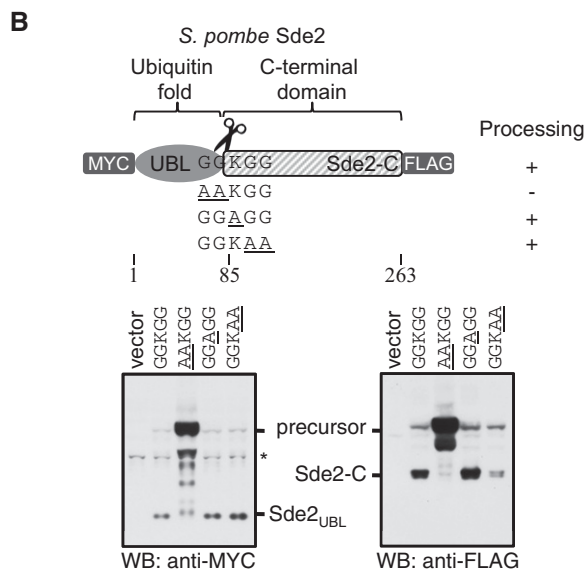
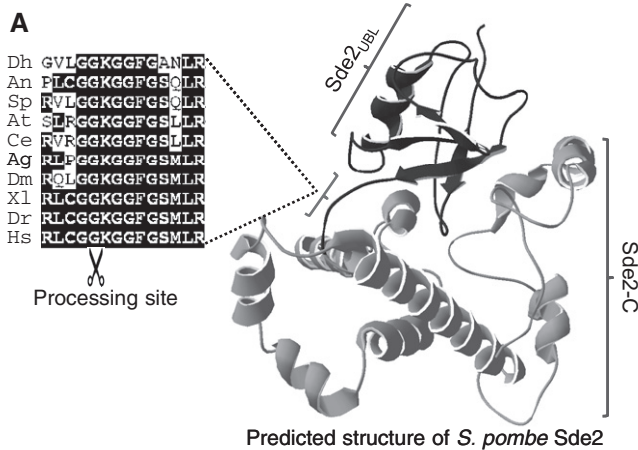
We generated a tagged version of Sde2, which contained epitope tags at both its N- and C-termini, to detect the protein in *S. pombe* by immunoblot assays. These experiments revealed that the full-length protein was cleaved, separating it into Sde2<sub>UBL</sub> and Sde2-C (Fig 1B). After processing, Sde2<sub>UBL</sub> was diffusely localized in *S. pombe* whereas Sde2-C was predominantly nuclear (Appendix Fig S1B). Processing of Sde2 is presumed to occur at the GG<sup>K</sup>GG sequence as alanine substitutions of the first GG residues abolished cleavage (Fig 1B) and a processing-defective Sde2 was nuclear (Appendix Fig S1B). Importantly, these alanine substitutions also failed to rescue growth defects of a  $\Delta sde2$  strain (Fig 1C), suggesting that cleavage of Sde2 is essential for its function. By contrast, alanine mutations of the lysine or the second GG residues had negligible effects on processing and these mutants also rescued growth defects of  $\Delta sde2$ , albeit to a lesser extent than the wild type. Sde2 must be synthesized in the precursor form that should get processed for function, as *de novo* expressions of Sde2<sub>UBL</sub> did not complement growth defects in  $\Delta sde2$  strain whereas Sde2-C complemented the defects partially after overexpression (level of Sde2-C when expressed from a plasmid using methionine codon was higher than Sde2-C generated from its chromosomal location; Appendix Fig S1C). Co-expression of the two domains did not improve growth of the deletion strain (Fig 1D). An extension with a non-cleavable peptide upstream of Sde2-C did not result in any complementation (Appendix Fig S1D). Thus, Sde2-C is the functional unit whereas Sde2<sub>UBL</sub> plays a regulatory role.

To examine evolutionary conservation of Sde2 processing, an epitope-tagged version of the human ortholog, C1orf55 (herein referred to as HsSde2) was generated. Similar to *S. pombe*, HsSde2 precursor was also cleaved into HsSde2<sub>UBL</sub> and HsSde2-C in mammalian cells, alanine mutations of the first GG residues in the GGKGG motif of HsSde2 abolished its processing, and mutation of the lysine did not have any visible effect on processing (Fig EV1D).

Interestingly, the HsSde2-C protein formed after processing of the GG<sub>AGG</sub> mutant precursor accumulated to higher levels than the protein formed from the wild-type precursor (Fig EV1D; see below). Nevertheless, despite the similar post-translational processing of Sde2 in *S. pombe* and humans, these orthologs retain organism-specific features, as expression of HsSde2 in *S. pombe*  $\Delta sde2$  strain failed to complement its growth defects. Furthermore, the two domains of HsSde2 were not interchangeable with the *S. pombe* counterparts, as a domain-swapped *S. pombe*-human Sde2 chimera could not complement  $\Delta sde2$  (Appendix Fig S1E).

### Ubiquitin-specific proteases Ubp5 and Ubp15 process Sde2

To identify Sde2 processing enzymes, we monitored accumulation of its precursor in selected mutants of *S. pombe* proteases by



immunoblot assays. The precursor accumulated in a strain lacking *ubp15*, a USP domain-containing DUB (Appendix Fig S2A). Residual Sde2-C in the  $\Delta ubp15$  strain suggested involvement of additional enzymes for the processing. It was previously reported that *ubp15*

**Figure 1. Sde2 is a conserved protein with ubiquitin-fold.**

**A** Predicted structure of *Schizosaccharomyces pombe* Sde2 protein shows the presence of a ubiquitin-fold (Sde2<sub>UBL</sub>) and a helical C-terminal domain (Sde2-C). The alignment on the left shows the linker GGGKGG motif between Sde2<sub>UBL</sub> and Sde2-C in Sde2 orthologs. Dh, *Debaryomyces hansenii*; An, *Aspergillus niger*; Sp, *Schizosaccharomyces pombe*; At, *Arabidopsis thaliana*; Ce, *Caenorhabditis elegans*; Ag, *Anopheles gambiae*; Dm, *Drosophila melanogaster*; Xl, *Xenopus laevis*; Dr, *Danio rario*; Hs, *Homo sapiens*.

**B** Expression and processing of Sde2 protein in *S. pombe* detected by immunoblot analysis (Western blot, WB) using epitope tag-specific antibodies. Underlined residues mark changes from wild-type (WT) Sde2. Asterisk indicates antibody cross reactivity signal.

**C** Complementation of *S. pombe*  $\Delta sde2$  by GGGKGG mutants of Sde2. Constructs are as in (B). Fivefold serial dilution spotting was done on indicated agar plates. Plates were incubated at 30°C and 37°C until growth appeared.

**D** Complementation of *S. pombe*  $\Delta sde2$  by Sde2 domains. The experiment is as in (C). Expression constructs encoding Sde2 WT, the processing-defective mutant sde2(AAKGG), Sde2<sub>UBL</sub>, Sde2-C, and Sde2<sub>UBL</sub> and Sde2-C together were used.

Source data are available online for this figure.

genetically interacts with *ubp5*, with the double mutant showing synthetic sickness (Richert *et al.*, 2002). Processing of Sde2 was completely abolished in a  $\Delta ubp5 \Delta ubp15$  double mutant (Fig 2A and B). To monitor sub-cellular location of Sde2 processing, we generated Sde2<sub>UBL</sub>-GFP chimera, with a nuclear localization signal (NLS) or a nuclear export signal (NES) at the C-terminus of GFP. An inefficient processing of the Sde2<sub>UBL</sub>-GFP-NES chimera in *S. pombe* suggests that Sde2 processing takes place in the nucleus (Fig 2C). Ubp5 and Ubp15 are generally involved in processing of ubiquitin and ubiquitin conjugates (Kouranti *et al.*, 2010), and clearly, Sde2 is not the only substrate of Ubp5 and Ubp15; accordingly, the  $\Delta ubp5 \Delta ubp15$  strain showed more severe growth defects than the  $\Delta sde2$  strain (Appendix Fig S2B).

To further test whether Ubp5 and Ubp15 acted directly as the proteases, we examined processing of *SpSde2* by these DUBs in the recombinant system of *Escherichia coli*. Efficient processing of Sde2 was readily observed in *E. coli* upon co-expression of Ubp5 and Ubp15, but not their catalytically inactive cysteine mutants (Fig 2D). Activity of these proteases on Sde2 is highly specific, as another USP domain-containing DUB, Ubp16, did not process Sde2 (Fig EV2A). Although *S. cerevisiae* lacks Sde2, it contains an Ubp15 ortholog. Nevertheless, *SpSde2* was poorly processed in wild-type *S. cerevisiae*, presumably because *SpUbp15* and *ScUbp15* share only 44% identity. Overexpression of *ScUbp15* enabled detection of processed *SpSde2*-C in *S. cerevisiae*. Importantly, increased efficiency of *SpSde2* processing was apparent upon co-expression of either *SpUbp5* or *SpUbp15* in *S. cerevisiae*, highlighting their roles in processing of *SpSde2* (Appendix Fig S2C).

We reasoned that if Sde2<sub>UBL</sub> was processed at the GG motif mainly for generating <sup>Lys</sup>Sde2-C, then it should be replaceable with UBLs that are similarly processed. Therefore, we generated fusions of Sde2-C with *S. pombe* ubiquitin, Ned8 (NEDD8 ortholog) or Hub1 (used here as a control UBL that is not processed). The GGGKGG sequence was kept at the junction of the chimera. Ubiquitin and Ned8, but not Hub1, chimeras of <sup>Lys</sup>Sde2-C complemented growth defects of the  $\Delta sde2$  strain (Fig EV2B). Ubiquitin- and Ned8-specific proteases processed respective fusions to form the functional <sup>Lys</sup>Sde2-C (Fig EV2C). Processing of ubiquitin-Sde2-C and Ned8-Sde2-C fusions was not affected in  $\Delta ubp5 \Delta ubp15$

double mutant (Fig EV2D). Since Hub1 does not get processed, its chimera was unable to generate functional Sde2-C. Similar to the processing-defective mutants of Sde2, alanine mutations of the GG in the chimeras were not processed and remained non-functional.

**Sde2-C is a substrate of the N-end rule pathway**

To monitor steady-state levels of wild-type and mutant Sde2 proteins, sequence encoding 6HA epitope tag was inserted chromosomally at the C-terminus of *sde2* variants. <sup>Met</sup>Sde2-C formed after processing of the GGMGG mutant precursor accumulated to higher levels than the <sup>Lys</sup>Sde2-C formed from the wild-type GGKGG protein (Fig 3A and B). Interestingly, the level of <sup>Met</sup>Sde2-C after *de novo* translation using methionine codon was lower than the <sup>Met</sup>Sde2-C formed after processing of the GGMGG mutant precursor. However, the differences in protein levels were not due to variations in transcription, as all strains showed comparable levels of *sde2* mRNA in reverse transcription quantitative PCR (RT-qPCR) assays (Appendix Fig S3A). Thus, the presence of Sde2<sub>UBL</sub> facilitates the expression of Sde2-C protein. Both strains with <sup>Met</sup>Sde2-C showed strong growth defects; however, growth of the strain with <sup>Met</sup>Sde2-C formed after processing of the GGMGG mutant was better than with <sup>Met</sup>Sde2-C from *de novo* translation (Fig 3C).

The lower levels of *S. pombe* and human <sup>Lys</sup>Sde2-C (Figs 3D and EV1D) could be because lysine residue at the amino-terminus of proteins is descriptive of a type 1 degron in the N-end rule pathway (Bachmair *et al*, 1986; Sriram *et al*, 2011). Thus, we tested whether Sde2-C was a substrate of this pathway by measuring its turnover rates. Indeed, the <sup>Lys</sup>Sde2-C protein was short-lived, whereas the <sup>Met</sup>Sde2-C proteins were significantly stabilized (Fig 3D). *Schizosaccharomyces pombe* deletion of the N-end rule ligase *ubr11* (Fujiwara *et al*, 2013) partially stabilized <sup>Lys</sup>Sde2-C (Appendix Fig S3B). The mutation of the 19S proteasome regulatory particle subunit *mts3* (Gordon *et al*, 1996) stabilized <sup>Lys</sup>Sde2-C, and higher molecular weight adducts of Sde2 observed in this mutant (Fig 3E) were confirmed to be ubiquitin conjugates of Sde2 by pull-down assays of the conjugates under denaturing conditions (Fig 3F). Ubiquitination of Sde2 was diminished but not abolished in a *Δubr11* strain (Appendix Fig S3C), indicating involvement of additional ligase(s) for degradation of Sde2-C.

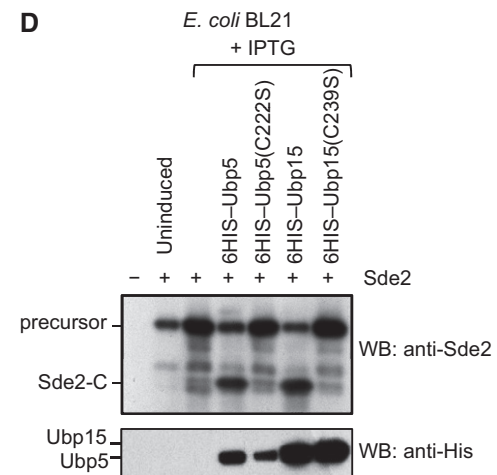
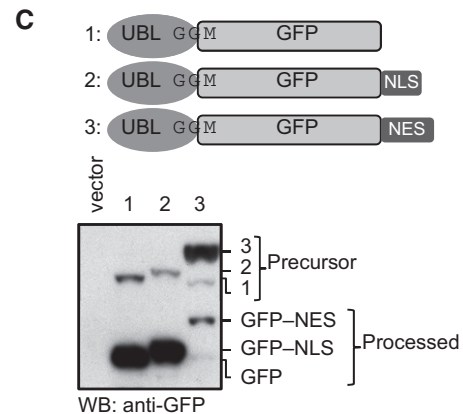
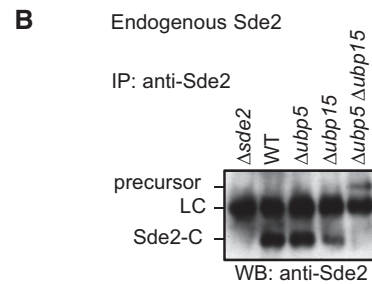
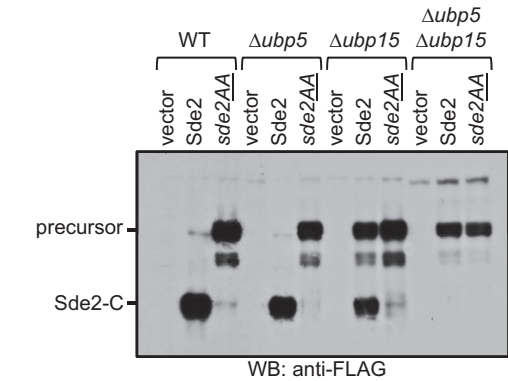


**Figure 2. Ubiquitin-specific proteases Ubp5 and Ubp15 process Sde2.**

- A Sde2 processing in *Schizosaccharomyces pombe*. Constructs from Fig 1B were expressed in *S. pombe* WT, *Δubp5*, *Δubp15* and *Δubp5 Δubp15* strains. The protein expression was analysed by anti-FLAG immunoblotting.
- B Endogenous *S. pombe* Sde2-C and the full-length Sde2 precursor in *Δubp5 Δubp15* strain. Sde2 protein from indicated strains was immunoprecipitated using a polyclonal antibody against recombinant Sde2-C, followed by Western blot analysis using same antibody.
- C Sde2 is processed in the nucleus. Anti-GFP immunoblot analysis of *S. pombe* expressing Sde2<sub>UBL</sub>-GFP, and its variants with a nuclear localization signal (NLS) or a nuclear export signal (NES). The non-nuclear NES version was poorly processed.
- D Processing of *S. pombe* Sde2 in bacteria. Expression constructs harbouring indicated cDNAs were co-transformed in *Escherichia coli* BL21(DE3) strain. Following protein expression, total cell lysates were processed by immunoblotting using anti-Sde2-C antibody. Anti-HIS immunoblotting was done to monitor expression of the proteases and its mutants.

Source data are available online for this figure.

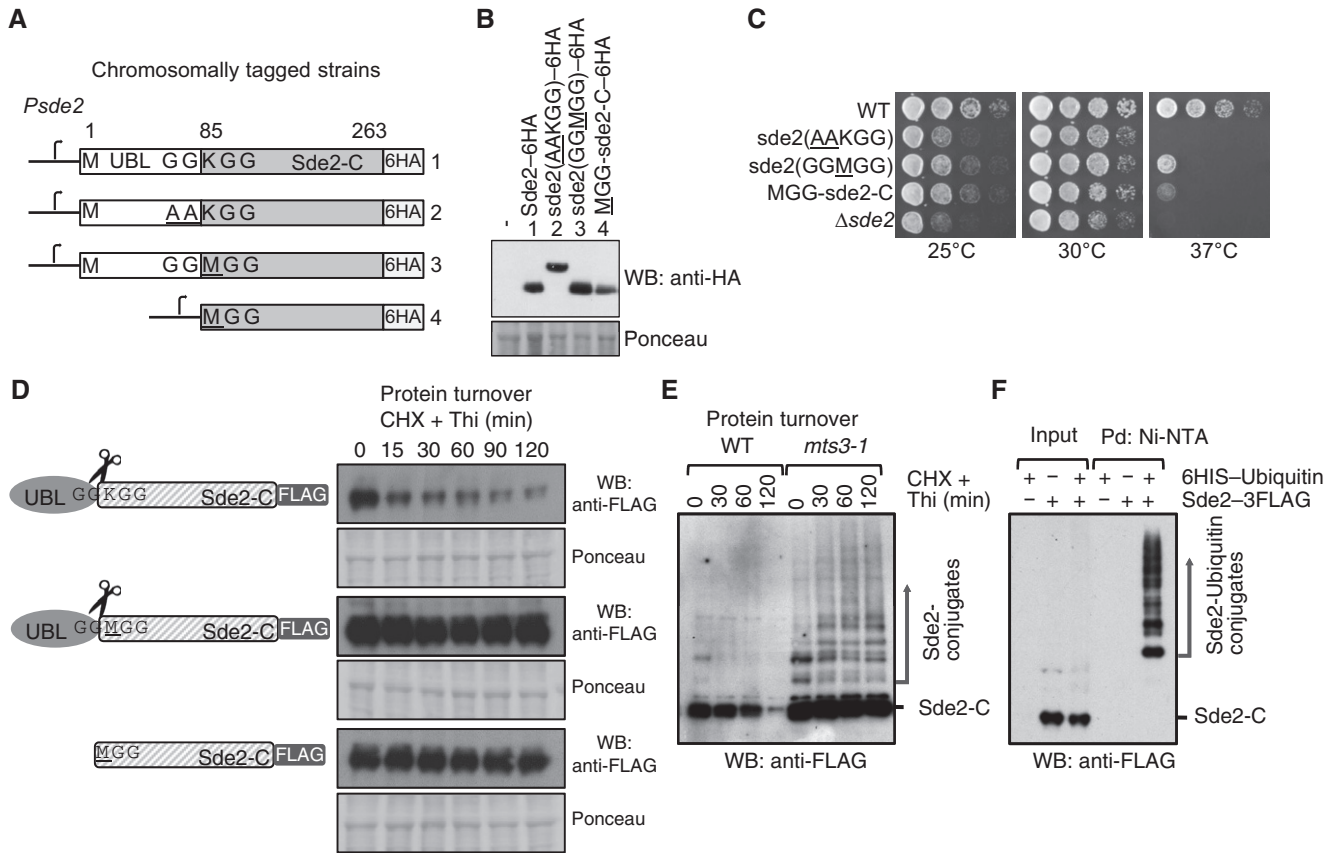


**Figure 3. Sde2-C is made short-lived by the N-end rule pathway.**

**A** Chromosomal 6HA epitope-tagged *sde2* variants. The *sde2* promoter is common to all variants.  
**B** Western blot with anti-HA antibody to detect steady-state levels of wild-type and mutant Sde2 proteins.  
**C** Growth phenotype of strains in (A). Strains with <sup>Met</sup>Sde2-C proteins, formed either after processing of GGMGG mutant or translated *de novo*, show  $\Delta sde2$ -like growth defects.  
**D** Constructs used to monitor steady-state level and turnover of the proteins. Plasmids contain 3FLAG epitope tags at the C-termini of Sde2 under *nmt81* promoter. Protein turnover assays. The Sde2 variants with C-terminal 3FLAG tag were expressed in  $\Delta sde2$  strain from a plasmid under *nmt81* promoter. In Sde2 WT, after processing Sde2-C starts with lysine, in GGMGG mutant with methionine and Met-Sde2-C is *de novo* translated. Total proteins from 1.0 OD<sub>600</sub> cells for the given time points were run on SDS-PAGE followed by anti-FLAG Western blotting.  
**E** WT Sde2 is stable in the proteasome mutant *mts3-1*. Assay is similar to (B). Higher molecular weight adducts detected with anti-FLAG antibody likely represent ubiquitinated Sde2.  
**F** Denaturing Ni-NTA pull-down (Pd) of ubiquitin conjugates from *Schizosaccharomyces pombe* expressing Sde2-3FLAG. Ubiquitination of Sde2 is detected by anti-FLAG immunoblotting.

Source data are available online for this figure.

To elucidate role of the conserved lysine in GGKGG motif in Sde2 orthologs, we generated substitution mutations with each of the other 19 amino acids and measured the processing efficiency, half-life and complementation capacity of each of the resulting proteins. All amino acid variants, excluding the version with a proline GGPPG, underwent efficient processing (Fig EV3; Appendix Fig S3D and E), indicating that the lysine is not required for processing. In assays to measure proteins half-life, the <sup>Met</sup>Sde2-C variant was found to be most stable, the <sup>Arg</sup>Sde2-C variant was the least stable, and the wild-type <sup>Lys</sup>Sde2-C had an intermediate stability. Function-wise, growth defects of the  $\Delta sde2$  strain could be best complemented by the wild-type <sup>Lys</sup>Sde2-C followed by the <sup>Trp</sup>Sde2-C and <sup>Gly</sup>Sde2-C variants. By contrast, the <sup>Cys</sup>Sde2-C, <sup>Glu</sup>Sde2-C and <sup>Asp</sup>Sde2-C variants showed the weakest complementation. The GGPPG mutant of Sde2 was

defective for processing and failed to complement  $\Delta sde2$  (Fig EV3; Appendix Fig S3D and E). Similar defects in the processing of a ubiquitin-proline- $\beta$ -galactosidase chimera were reported in *S. cerevisiae* (Bachmair et al, 1986). Thus, the N-end rule pathway controls the levels of <sup>Lys</sup>Sde2-C by its turnover in the proteasome.

**Processing of Sde2<sub>UBL</sub> promotes association of Sde2-C with the spliceosome**

To better understand the cellular role of Sde2, mass spectrometry was used to identify proteins that co-immunoprecipitated (Co-IP) with an epitope-tagged version of Sde2 (Appendix Fig S4A). Here, we confirmed association between Sde2 and components of the spliceosome, as recently reported by others (Bayne et al, 2014; Chen

et al, 2014). Co-IP assays using chromosomally epitope-tagged versions of multiple Cdc5/Prp19 complex subunits, including Cdc5, Prp19 and Isy1, further validated these interactions (Fig 4A). Notably, the level of Sde2 protein detected in these experiments appears lower than the subunits of the Cdc5 complex (Appendix Fig S4B), suggesting that Sde2 functions substoichiometrically within the spliceosome.

We tested the ability of processing-defective and lysine mutants of Sde2 for interaction/incorporation in spliceosomes. For this purpose, we performed Co-IP assays of these mutants with core spliceosomal factors Cdc5 and Cwf21. To test the interaction at the endogenous levels of the proteins, we chromosomally inserted a sequence encoding 9MYC epitope tag at the C-terminus of Cdc5 and Cwf21 in the chromosomal Sde2–6HA variants shown in Fig 3A. By contrast to the <sup>Lys</sup>Sde2-C, which associated efficiently with Cdc5 and Cwf21, Co-IP of the precursor AAKGG was strongly diminished (Fig 4B and C). Since Sde2 in the AAKGG strain remains mainly in the precursor form, the residual spliceosomal association of this precursor (Fig 4B and C) might have happened because of the lack of active Sde2-C. To address this, we performed Cdc5 Co-IP of a partially processed GAKGG mutant of Sde2, which produces similar levels of precursor and processed proteins; herein, only the processed Sde2-C associated with Cdc5 (Fig EV4). Thus, spliceosomal association of a small amount of Sde2 precursor is possible, but only in the absence of processed Sde2-C. Moreover, Sde2<sub>UBL</sub> appears inhibitory for the precursor's association with the spliceosome, as Cdc5 Co-IP of free <sup>Met</sup>Sde2-C, formed either after processing of the GGMGG precursor or from *de novo* translation, remained largely unaffected (Fig 4D). These results suggested that processing of Sde2<sub>UBL</sub> facilitates incorporation of <sup>Lys</sup>Sde2-C in the spliceosome, wherein the conserved lysine may not be critical for this association.

**Sde2-C is an intron-specific pre-mRNA splicing factor**

To elucidate the role of Sde2 in pre-mRNA splicing, we analysed splicing defects in  $\Delta sde2$  strain using *S. pombe* genome-wide

splicing-sensitive microarrays (Inada & Pleiss, 2010). The arrays have oligonucleotide probes specific for exons, introns and exon–exon junctions for nearly all intron-containing genes in *S. pombe*. Since the  $\Delta sde2$  strain showed temperature-sensitive growth defects, we analysed cells grown at 30°C or after shifting to 37°C for 15 min to detect early splicing defects. As seen in Fig 5A, splicing of most intron was unaffected in  $\Delta sde2$  strain under either growth condition, as evidenced by the lack of apparent changes in pre-mRNA levels. Interestingly, however, splicing defects were observed for nearly 30

**Figure 4. Processing of Sde2<sub>UBL</sub> promotes interaction of Sde2-C with the spliceosomal factors.**

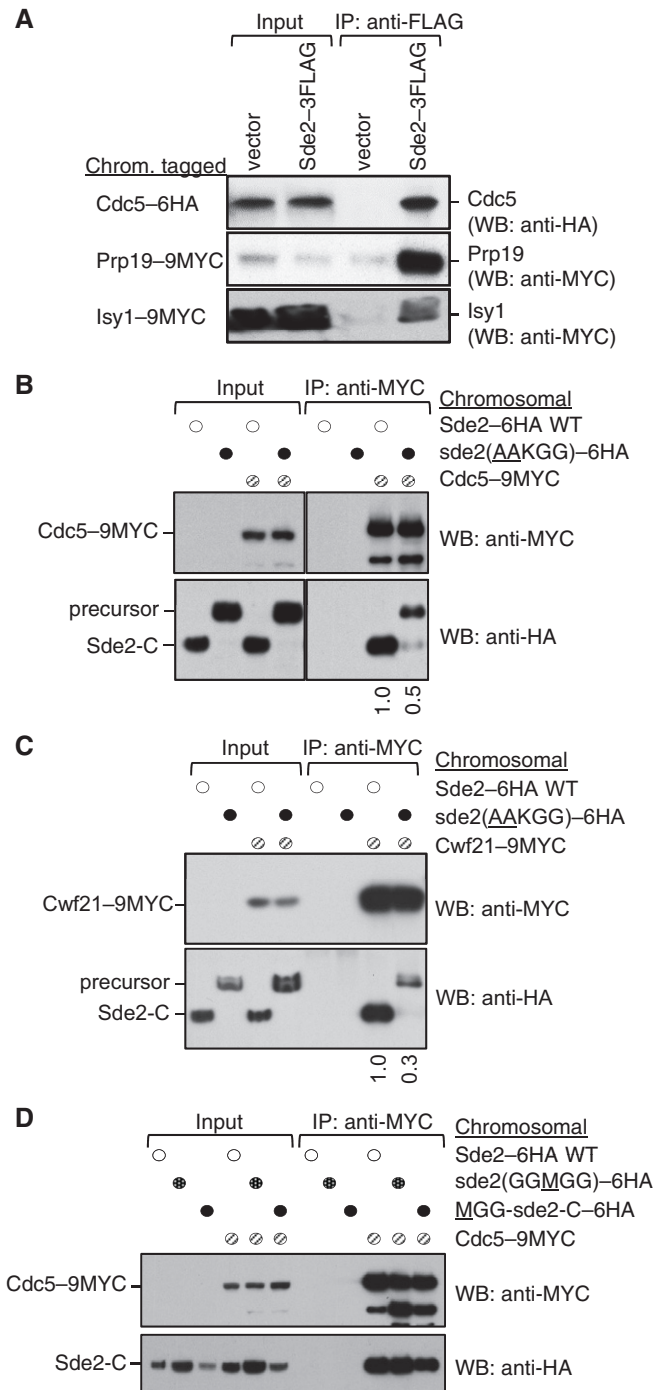
A Sde2 interacts with the spliceosomal Prp19 complex factors Cdc5, Prp19 and Isy1 *in vivo*. *sde2* gene was 3FLAG-tagged, and *cdc5-6HA*, *prp19-9MYC* and *isy1-9MYC* genes were tagged chromosomally.

B Co-IP assay to monitor association of the processing-defective Sde2 with Cdc5. Experiments are performed with proteins expressed at their endogenous levels by using chromosomally tagged strains with given epitopes at the C-termini of indicated genes. IP was performed using anti-MYC agarose resins followed by immunoblot assays with anti-MYC antibody to monitor IP efficiency of Cdc5, and with anti-HA antibody to monitor Co-IP of Sde2 versions. Numbers below anti-HA blot indicate ratio of Sde2 to Cdc5 (HA/MYC) signals obtained from ImageJ quantification of immunoblot signals. Cdc5 association of the processing-defective Sde2 precursor is diminished to half.

C Co-IP assay to monitor association of the processing-defective Sde2 with Cwf21. Assay is similar to (B). Cwf21 association of the processing-defective Sde2 precursor is diminished to one-third.

D Co-IP assay to monitor association of <sup>Met</sup>Sde2-C with Cdc5. Assay and quantitation is similar to (B). <sup>Met</sup>Sde2-C generated from processing of GGMGG mutant precursor or after translation *de novo* does not show obvious defects in spliceosomal association.

Source data are available online for this figure.



genes, where pre-mRNA levels were increased by at least twofold, and were often accompanied by decrease in the levels of mature mRNA (Fig 5A inset).

We confirmed splicing defects of selected candidates in  $\Delta sde2$  by RT-PCR assays, followed by agarose gel electrophoresis to visualize intron-containing transcripts (Fig 5B; Appendix Fig S5A and B). Key targets of Sde2 include multi-intronic genes *rap1* (encodes a telomere binding protein with functions in telomeric silencing), *psf3* (encodes a GINS complex subunit with functions in DNA replication), and *mcs2* (encodes a TFIIF complex cyclin with functions in transcription). Strikingly, for all these targets one of the RT-PCR bands in  $\Delta sde2$  sample could not correspond to the products expected from either fully spliced or fully unspliced mRNAs. Consistent with the array analysis for these targets (Table EV1), gel-purification and sequencing of these bands showed transcripts having retained only one of the intron (for *rap1* intron-2, *psf3* intron-4, and *mcs2* intron-2), accumulated in  $\Delta sde2$  (Fig 5B; Appendix Fig S5C). The Sde2-C target introns are enriched with non-canonical 5'- and 3'-splice sites (Table EV2). Nevertheless, a common feature or sequence element was not obvious in affected pre-mRNAs or introns. The respective cDNAs of the three targets could not complement growth defects of  $\Delta sde2$  strain (Appendix Fig S5D); thus, the defects appear to have arisen from cumulative splicing defects of multiple targets.

The *hub1-1* mutant defective in pre-mRNA splicing (Mishra et al, 2011) showed distinct splicing defects for above transcripts, as different introns of *mcs2* and *rap1* were retained in this mutant (Fig EV5A). Thus, Sde2 and Hub1 do not seem to have overlapping functions in pre-mRNA splicing, and the negative genetic interaction between their mutants (Fig EV1A and B) likely resulted from splicing defects of a larger number of transcripts in the double mutant. We reasoned that since <sup>Lys</sup>Sde2-C has rapid turnover rate, overexpression of its stable versions could be toxic and/or dominant-negative in the cell. Indeed, overexpression of <sup>Met</sup>Sde2-C or <sup>Ala</sup>Sde2-C proteins resulted in slow growth phenotypes in *hub1-1* strain (Appendix Fig S6A). This phenotype seems to arise from  $\Delta sde2$ -like pre-mRNA splicing defects in *hub1-1* strain (Appendix Fig S6B) indicating that stable forms of Sde2 are dominant-negative in the cell.

**Sde2 processing is needed for telomeric silencing and genome stability**

A functional link between Sde2 and its proteases Ubp5/Ubp15 for intron-specific pre-mRNA splicing was confirmed from  $\Delta sde2$ -like splicing defects observed in the deletion strain of the proteases (Fig 6A). The processing of Sde2 precursor and the lysine at the N-terminus of Sde2-C both are essential for the splicing function, as

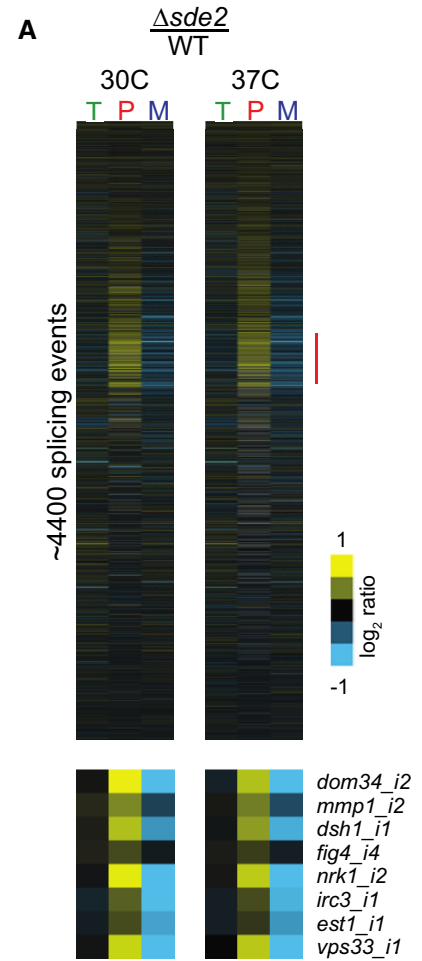
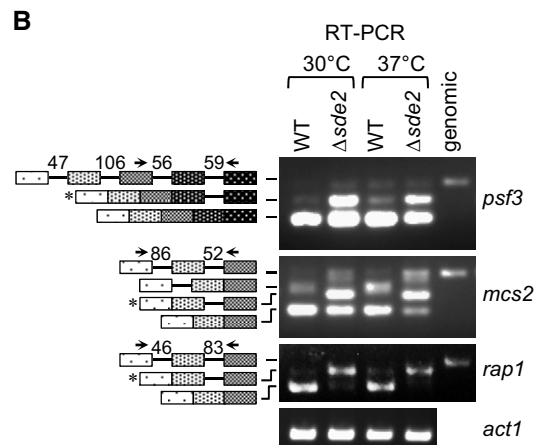


**Figure 5. Sde2 is required for excision of selected introns from a subset of pre-mRNAs.**

**A** Analysis of total RNA from *Schizosaccharomyces pombe* WT and  $\Delta sde2$  strain using splicing-sensitive microarray. Microarray heat-map shows  $\log_2 \Delta sde2/WT$  ratio of signals for total transcripts (T), intron-containing transcripts (P) and spliced transcripts (M). 37°C temperature shift was performed for 15 min to monitor early splicing defects. The experiment was repeated with dyes swapped. Yellow colour represents accumulation, black denotes no change, and blue shows reduction of signal in  $\Delta sde2$ .

**B** Semi-quantitative RT-PCR shows intron-containing transcripts for *psf3*, *mcs2* and *rap1*. cDNA prepared from total RNA isolated from *S. pombe* WT and  $\Delta sde2$  mutant at 30°C and 37°C was analysed by PCR. The block diagram (not drawn to the scale) shows exons and introns. Arrows mark primers used for amplification. The numbers above introns (shown as lines in block diagrams) mark their lengths. PCR band from genomic DNA (genomic) corresponds to the pre-mRNA. RT-PCR of *act1* (actin) pre-mRNA is used as control. Asterisks mark intron-containing transcripts getting enriched in  $\Delta sde2$ .

Source data are available online for this figure.



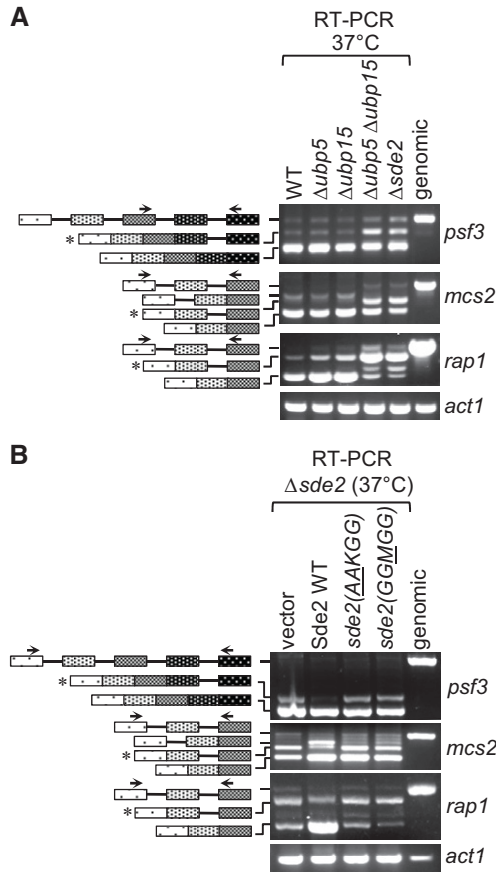


**Figure 6. Sde2 processing in pre-mRNA splicing.**

A  $\Delta sde2$ -like intron-specific splicing defect in  $\Delta ubp5 \Delta ubp15$  mutants defective in Sde2 processing. The details are as in Fig 5B.  
 B Intron-specific splicing defects in processing-defective and lysine mutants of Sde2. *Schizosaccharomyces pombe*  $\Delta sde2$  strain was transformed with vector, Sde2 WT, *sde2(AAKGG)* and *sde2(GGMGG)*. The details are as in Fig 5B.  
 Source data are available online for this figure.

respective mutants also had  $\Delta sde2$ -like splicing defects (Fig 6B). Sde2-specific function in telomeric silencing and mini-chromosome stability was reported previously (Sugioka-Sugiyama & Sugiyama, 2011). Supporting a role for Sde2 in telomeric silencing, we observed aberrant overexpression of the telomeric DNA helicases *tlh1*, *tlh2* and *SPAC212.06c* in  $\Delta sde2$  in our microarrays, which was further confirmed by RT-qPCR assays (Fig 7A). As expected from the small in number yet functionally related targets of Sde2, the defects in telomeric silencing in Sde2 mutants could not be assigned to the splicing defect of a single gene (Appendix Fig S7B and C; Table EV1 and online microarray data). Importantly, the processing-defective and lysine mutants of Sde2 also showed  $\Delta sde2$ -like defects in telomeric silencing and mini-chromosome stability assays (Fig 7B and C), thus revealing a role of ubiquitin-like processing for intron-specific pre-mRNA splicing and associated telomeric silencing and genomic stability.

**Sde2-C facilitates association of Cay1 with spliceosomes**

To understand the mechanism of Sde2 in the spliceosome, we purified and compared spliceosomes from wild-type and  $\Delta sde2$  strains

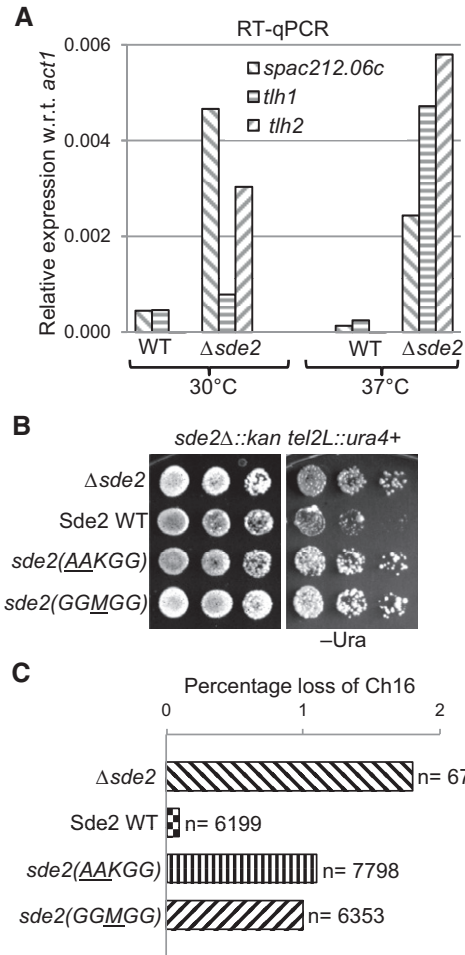


**Figure 7. Sde2 processing in telomeric silencing and genome stability.**

A Aberrant overexpression of telomeric transcripts in Sde2 mutant. Expression levels of telomeric transcripts *tlh1*, *tlh2* and *SPAC212.06c* were quantitated by RT-qPCR assays in WT, and  $\Delta sde2$  strain at 30°C and 37°C is normalized with *act1*.  
 B Telomeric silencing assay in Sde2 mutants. *ura4+* gene inserted at the telomere in  $\Delta sde2$  strain (Sugioka-Sugiyama & Sugiyama, 2011) was used as a marker to assay telomeric silencing on indicated agar plates. Suppression of growth on -Ura plate indicates silencing of the reporter at the telomeres.  
 C Mitotic chromosome stability assay to assess genomic instability in Sde2 mutants. Percentage loss of chromosome 16 in  $\Delta sde2$  strain (Sugioka-Sugiyama & Sugiyama, 2011) transformed with Sde2 variants is plotted (*n* = total number of colonies counted). Processing-defective and lysine mutants of Sde2 show elevated loss of the chromosome.  
 Source data are available online for this figure.

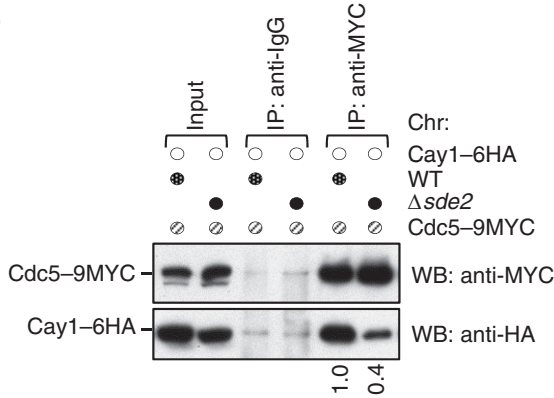
harbouring chromosomal Cdc5-6HA and Prp19-6HA tags by mass spectrometry. We found that, whereas the composition of spliceosomes in the two strains was almost identical, peptides for Cactin/Cay1 were diminished in spliceosomal purifications from  $\Delta sde2$  strains (Fig 8A; Table EV3). We confirmed Sde2-C dependent association of Cay1 with spliceosomes by Co-IP experiments (Fig 8B). An epistatic relationship between *sde2* and *cay1* (Fig 8C) and similar pre-mRNA splicing defects in single and double mutants (Fig 8D) suggest that Cactin also functions as an intron-specific splicing regulator. A role of *S. pombe* Cactin in splicing of *rap1* pre-mRNA was



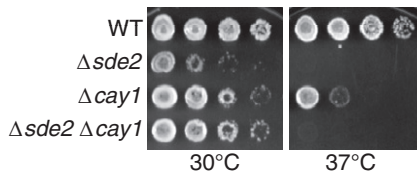
**A Unique peptides in mass spectrometry**

Protein	IP: Sde2-6HA		IP: Cdc5-6HA		IP: Prp19-6HA	
	WT	$\Delta sde2$	WT	$\Delta sde2$	WT	$\Delta sde2$
Cdc5	61	72	74	69	69	69
Prp19	25	28	28	26	23	23
Cay1	26	15	9	9	1	1

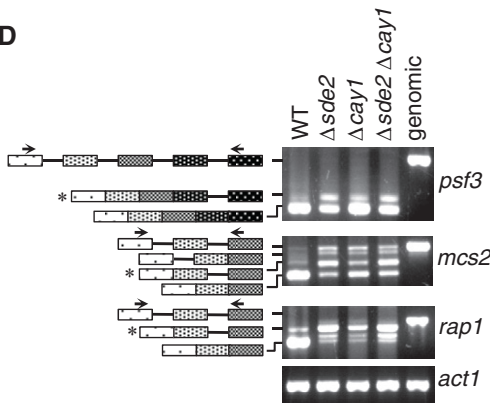
**B**



**C**



**D**



**E**

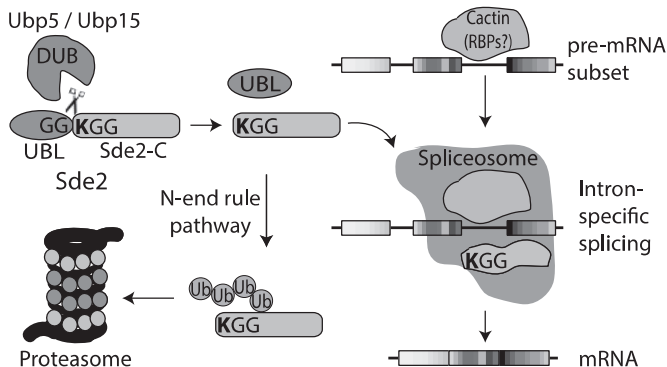


**Figure 8. Sde2-C facilitates association of Cay1 with spliceosomes.**

**A** Sde2 Co-IPs with Cactin in the spliceosome. Cdc5-6HA and Prp19-6HA complexes were immunoprecipitated using anti-HA antibody beads from *Schizosaccharomyces pombe* lysates wild-type and  $\Delta sde2$  strains. Co-IP proteins were analysed by mass spectrometry. The table shows number of unique peptides obtained for each protein in mass spectrometry.

**B** Sde2 facilitates recruitment of Cay1 to the spliceosome. Assay is similar to (A). Lysates from *S. pombe* wild-type and  $\Delta sde2$  strain with Cdc5-9MYC and Cay1-6HA tagged were immunoprecipitated using anti-MYC antibody beads. Co-IP of Cay1-6HA was analysed by anti-HA Western blot. Numbers below anti-HA blot indicate ratio of Cay1 to Cdc5 (HA/MYC) signals obtained from ImageJ quantification of immunoblot signals.

**C** Sde2 and Cay1 are epistatic. Fivefold serial dilution spotting of indicated mutant strains was done on rich media. Plates were incubated at 30°C and 37°C until growth appeared.

**D** Cay1 and Sde2 knockout strains have similar pre-mRNA splicing defects. Assay is similar as in Fig 5B.

**E** Schematics for Sde2 function and regulation.

Source data are available online for this figure.

reported (Lorenzi *et al*, 2015), but its spliceosomal association and intron-specific splicing function was not uncovered.

Turnover rates of lysine mutants of <sup>Lys</sup>Sde2-C did not correlate well with their ability to complement growth defects in  $\Delta sde2$  strain (Fig EV3). While the lysine was not critical for the association of Sde2-C with spliceosomes (Fig 4D), we tested whether the lysine is needed for specific association with Cay1. Indeed, Co-IP of Cay1 with <sup>Met</sup>Sde2-C was strongly diminished and with <sup>Arg</sup>Sde2-C and <sup>Thr</sup>Sde2-C was weaker than the wild-type <sup>Lys</sup>Sde2-C (Fig EV5B and C). Thus, the extent of complementation of  $\Delta sde2$  by the lysine mutants of Sde2-C appears to result from two activities, turnover by the N-end rule pathway and ability to associate with specific pre-mRNA splicing factors (Fig 8E).

**Discussion**

**The DUBs with dual specificity for Sde2<sub>UBL</sub> and ubiquitin**

We have found that the cell has used ubiquitin-like processing to obtain an intron-specific pre-mRNA splicing regulator, which needs to have a non-methionine amino acid as its amino end. Multiple lines of evidences confirmed that Sde2 is a *bona fide* UBL. First, the Sde2<sub>UBLGG</sub>-Sde2-C precursor is cleaved at the di-glycine motif by USPs Ubp5 and Ubp15. Second, Sde2<sub>UBLGG</sub>-GFP fusions were processed like Sde2 precursor. Third, cleavable ubiquitin and Ned8 could functionally replace Sde2<sub>UBL</sub>, whereas the processing-deficient UBL Hub1 could not.

The paralogs Ubp5 and Ubp15 are the two MATH/TRAF domain-containing ubiquitin proteases in *S. pombe*, which were reported to process ubiquitin. These proteases display a dynamic localization pattern in the Golgi, cytosol and nucleus (Kouranti *et al*, 2010). Since Sde2 is processed in the nucleus, the nuclear pool of these proteases would be more relevant for the activation of Sde2. The human ortholog of these DUBs, USP7/HAUSP, was reported to deubiquitinate and stabilize the tumour suppressor p53 (Li *et al*, 2002; Faesen *et al*, 2011) and its E3 ubiquitin ligase Mdm2 (Li *et al*, 2004). Their activities for both ubiquitin and Sde2 clearly show that both DUBs possess dual substrate specificity and process two distant UBLs with sequence identity less than 20%. The complete loss of

Sde2 processing in *S. pombe* deleted of *ubp5* and *ubp15* highlights specificity of this process, as other nuclear DUBs could not cleave Sde2<sub>UBL</sub>. The intriguing activity of Ubp5 and Ubp15 to process two distant UBLs requires structural studies of Sde2<sub>UBL</sub>-protease complexes to reveal the mechanism of catalysis. In support of conservation of Sde2 processing, Kim and colleagues have recently reported cleavage and degradation of human Sde2 in a PCNA-dependent manner and its role in replication stress (Jo *et al*, 2016).

### Sde2 precursor is similar to yet distinct from ubiquitin-ribosomal fusions

Sde2<sub>UBL</sub> and its processing are important for proper expression of the spliceosomal Sde2-C. This activity of Sde2<sub>UBL</sub> in the nucleus resembles the chaperone-like function of ubiquitin for the expression of ribosomal moieties from ubiquitin-ribosomal fusion proteins in the cytoplasm (Finley *et al*, 1989; Graciet *et al*, 2006; Lacombe *et al*, 2009). As Sde2<sub>UBL</sub> can be replaced with ubiquitin and Ned8, Sde2<sub>UBL</sub> function appears to be dedicated to generate the spliceosomal L<sup>ys</sup>Sde2-C. Although a common chaperone-like activity for all the three UBLs cannot be ruled out, this interpretation needs further investigation. We have not detected any higher molecular weight adducts of *S. pombe* Sde2<sub>UBL</sub>, but non-covalent functions of this UBL may exist in the cell.

The distinguishing feature of Sde2 orthologs is the conserved GGKGG motif, which is required for both processing and function. Processing of Sde2<sub>UBL</sub> has an activating role, as it is critical for interaction of L<sup>ys</sup>Sde2-C with spliceosomes. Activated L<sup>ys</sup>Sde2-C facilitates association of spliceosomes with Cactin/Cay1, a spliceosomal factor with Sde2-like function in intron-specific pre-mRNA splicing. While the lysine does not appear crucial for the interaction of L<sup>ys</sup>Sde2-C with spliceosomes, the residue is important for interactions with Cactin. The free lysine in L<sup>ys</sup>Sde2-C also plays a regulatory role, as it makes the protein a natural substrate of the N-end rule pathway of proteasomal degradation. Role of *S. pombe* Cactin for splicing of *rap1* pre-mRNA was reported previously (Lorenzi *et al*, 2015). Human Cactin functions in pre-mRNA splicing through interactions with splicing factors DHX8 and SRRM2 (Zanini *et al*, 2017). Cactin orthologs were detected in spliceosomal purifications (Bessonov *et al*, 2008; Doherty *et al*, 2014), and it also appears to have mRNAs binding ability (Baltz *et al*, 2012). Cactin possibly recognizes selected pre-mRNAs and facilitates their splicing with Sde2-C containing spliceosomes. The lysine has been selected for optimum function and interaction of Sde2-C in the spliceosome, as proteins neither with stabilizing residues nor with more destabilizing residues performed better than the wild type. To fine balance L<sup>ys</sup>Sde2-C level, the proteasome likely clears off non-spliceosomal pool of the protein by the N-end rule pathway.

### L<sup>ys</sup>Sde2-C is a unique pre-mRNA splicing regulator

L<sup>ys</sup>Sde2-C appears to function differently from other pre-mRNA splicing regulators of the spliceosome. L<sup>ys</sup>Sde2-C promotes efficient excision of selected introns from selected transcripts in *S. pombe*, but it is not required for general pre-mRNA splicing. L<sup>ys</sup>Sde2-C thereby becomes a critical control factor for the expression of selected proteins, a majority of which function at the chromatin. Therefore, growth defects or drug sensitivities of  $\Delta$ *sde2* strain could

not be attributed to splicing defects of individual genes. The lack of any obvious common feature in Sde2 target pre-mRNAs leads us to postulate that some RNA secondary structures could make their splicing Sde2 dependent. Importantly, Sde2-specific proteases play a key regulatory role in pre-mRNA splicing by processing the inactive Sde2 precursor to generate the active spliceosomal L<sup>ys</sup>Sde2-C, as Sde2<sub>UBL</sub> is inhibitory for its incorporation into the spliceosome. The processing-deficient and lysine mutants of Sde2 display  $\Delta$ *sde2*-like pre-mRNA splicing defect as well as defects in telomeric silencing and chromosome stability.

Splicing defects of a subset of pre-mRNAs were reported in the deletion strain of *tls1* (Wang *et al*, 2014). Specific pre-mRNA splicing defects have also been reported for mutants of U1 snRNA gene (Alvarez *et al*, 1996), U2AF, *prp18* and survival of motor neuron (SMN) gene (Webb *et al*, 2005; Campion *et al*, 2010; Vijaykrishna *et al*, 2016). We have previously reported an intron-specific pre-mRNA splicing defect of *cdc2* intron-3 in a *hub1* mutant of *S. pombe* (Mishra *et al*, 2011). Nevertheless, splicing targets of above factors are distinct, and respective gene deletions in *S. pombe* are inviable; thus, these factors are likely to be important for general pre-mRNA splicing. Interestingly, Sde2 orthologs could not be detected in intron-poor yeasts; therefore, it is tempting to propose that intron-loss during evolution (Hooks *et al*, 2014) might have resulted in the loss of Sde2 from these organisms.

In conclusion, the ubiquitin-like processing of Sde2<sub>UBL</sub> generates the activated L<sup>ys</sup>Sde2-C protein, which becomes functional in the spliceosome and plays a critical and selective role in pre-mRNA splicing. This process bears intriguing analogy to the processing of ubiquitin precursors with ribosomal proteins. Thus, the occurrence of precursors with ubiquitin-folds appears to be a conserved principle for both the ribosome and the spliceosome—the two major RNP complexes known to have certain similarities in their mechanisms of action (Konarska & Query, 2005; Staley & Woolford, 2009). Extending our current findings with Sde2, it is tempting to postulate that ubiquitin processing activates the ribosomal proteins for translation of selective mRNAs.

## Materials and Methods

### Strains, plasmids and DNA techniques

*Schizosaccharomyces pombe* strains used in this study are listed in Appendix Table S1, and plasmids are listed in Appendix Table S2. Strains for centromeric and telomeric silencing and mitotic chromosome loss assays in  $\Delta$ *sde2* strain were reported previously (Sugioka-Sugiyama & Sugiyama, 2011) and obtained from NBRP-yeast, Japan. Preparation of *S. pombe* competent cells, transformation, chromosomal tagging, gene deletion and isolation of total proteins for Western blot (WB; also referred to as immunoblot) assays by trichloroacetic acid (TCA) precipitation method was done following published protocols for *S. cerevisiae* (Knop *et al*, 1999; Janke *et al*, 2004). For growth and complementation assays, fivefold serial dilutions of cells were spotted on indicated agar plates until growth was seen. *Schizosaccharomyces pombe* expression constructs under a weak thiamine-repressible promoter *nmt81*, with sequences encoding 3MYC epitope tag at the N-terminus of *sde2* gene and 3FLAG epitope tag at its C-terminus, were used. The expression and

processing of the protein were analysed by anti-MYC and anti-FLAG immunoblotting. The promoter is induced in the absence of thiamine, and 5 µg/ml thiamine was used to repress the promoter. To shuffle-out *ura4<sup>+</sup>* plasmids from *S. pombe*, 5-fluoroorotic acid (FOA; Zymo Research) (1.0 g/l of media) was used in agar plates. Vectors for complementation assays were under the weak thiamine-repressible promoter *nmf1*. Plasmids with point mutations, insertions or deletions were created by QuikChange site-directed mutagenesis (Agilent) using specific primers. Gene fusions and chimeras were made by overlap extension (SOE) PCR method.

### Chromosomal mutagenesis of *sde2* gene

A plasmid was made which contained a NotI insert comprising of 500-bp *sde2* promoter, *sde2* ORF with the coding sequence of 6HA epitope tag, nat-NT2 cassette for resistance against Nat antibiotic, and 500 bp of *sde2* terminator. The plasmid was mutagenized by site-directed mutagenesis to obtain AAKGG and GGMGG, GGRGG and GGTGG versions of *sde2*. To obtain *MGG-sde2-C*, the sequence encoding amino acids 2–85 of *sde2<sub>UBL</sub>* was deleted by SOE PCR. The NotI inserts from the plasmids were purified and transformed in *Schizosaccharomyces pombe* strains followed by selection on YES-Nat plates. The chromosomal mutations were screened by growth phenotypes, immunoblotting assays using anti-HA antibody and/or sequencing of genomic PCR fragments covering the mutated regions.

### Protein immunoblot and turnover assays

For immunoblot assays, total protein isolated from logarithmically growing 1.0 OD<sub>600</sub> cells by TCA precipitation was separated on SDS-PAGE and transferred on PVDF membrane. To induce protein expression from thiamine-repressible *nmf* promoters, cells were first grown as primary cultures in the presence of 1.7 µg/ml thiamine. Protein expression was induced by growing the cultures in the absence of thiamine for 18–20 h at 30°C. For protein turnover assays, logarithmically growing cells at OD<sub>600</sub> = 0.7–0.8 were incubated for indicated time points with 1.7 µg/ml thiamine to repress the promoter, and 100 µg/ml of cycloheximide to stop protein translation. Total protein isolated from 1.0 OD<sub>600</sub> cells was used to monitor turnover of the protein by immunoblotting.

### Antibodies and antibody-coupled beads

The antibodies anti-haemagglutinin (HA, Clone HA-7), anti-HA (polyclonal), anti-Myc (polyclonal), anti-Flag M2 (Clone M2), anti-mouse-HRP and anti-rabbit-HRP (raised in Goat) were obtained from Sigma-Aldrich. Antibody-coupled beads were also from same source. Polyclonal antibody against bacterially purified GST-tagged Sde2-C was raised in rabbit (MERCK), and coupled to protein A/G beads (Pierce) for immunoprecipitation experiments.

### Screening for Sde2-specific proteases

*Schizosaccharomyces pombe* deletion strains of selected proteases from a haploid deletion library (Bioneer) were transformed with *pREP81x-3MYC-sde2-3FLAG* plasmid. The transformants were grown for 20 h in the absence of thiamine in EMM-Leu media. 1.0

OD<sub>600</sub> cells were harvested from logarithmically growing cultures and processed for immunoblot analysis.

### Processing of *Schizosaccharomyces pombe* Sde2 in *Escherichia coli* and *Saccharomyces cerevisiae*

*Escherichia coli* BL21(DE3) strain was used to monitor Sde2 processing with Ubp5 and Ubp15. For all co-transformations, *pPROEX-6HIS-Spsde2* plasmid was used with *pCDFduet empty*, *pCDFduet-6HIS-Spubp5*, *pCDFduet-6HIS-Spubp5(C222S)*, *pCDFduet-6HIS-Spubp15* and *pCDFduet-6HIS-Spubp15(C239S)*. Protein expression was induced in logarithmically growing cells using 100 µM IPTG for 16 h at 18°C. 1.0 OD<sub>600</sub> cells each were harvested and lysed for 10 min with 240 µl B-PER reagent (Pierce) containing benzonase (Sigma), 1 mM PMSF (Sigma) and protease inhibitor cocktail (Pierce). Sde2 was detected by anti-Sde2 immunoblotting. *Saccharomyces cerevisiae* PJ697a strain was used to monitor processing of *S. pombe* Sde2. *p426ADH-3MYC-Spsde2-3FLAG* plasmid was co-transformed with *p424ADH-Scubp15*, *p424ADH-Spubp5*, *p424ADH-Spubp5(C222S)*, *p424ADH-Spubp15*, *p424ADH-Spubp15(C239S)* plasmids. Co-transformants were grown in SC-Ura-Trp minimal media at 30°C. 1.0 OD<sub>600</sub> cells were harvested from logarithmically growing cells, processed by TCA prep and analysed by anti-FLAG immunoblotting.

### Co-immunoprecipitation (Co-IP) assays

The *in vivo* complex of Sde2 was analysed by immunoprecipitation (IP) of Sde2 complexes followed by mass spectrometry or by Co-IP assay from chromosomally tagged *S. pombe* strains. The assay was described previously (Mishra et al, 2011). For IP of Sde2 for mass spectrometry, *Δsde2* strain was transformed with *pREP81x-3MYC-sde2-3FLAG*. 500 OD<sub>600</sub> cells from exponentially growing culture were harvested. Primary cultures were grown in synthetic complete media then transferred to secondary culture in EMM-Leu media and finally to tertiary culture in EMM-Leu. 50 OD<sub>600</sub> cells were used for Co-IP assays. Total cell lysates were prepared by mechanical grinding with liquid nitrogen in the presence of cell-lysis buffer containing 50 mM Tris (pH7.5), 150 mM NaCl, 5 mM MgCl<sub>2</sub>, 5% glycerol, 1% Triton X-100, 1 mM PMSF (Sigma), phosphatase inhibitors (Roche) and protease inhibitors (Thermo Scientific). Lysates were cleared from cell debris by centrifugation at 10,000 × g for 10 min. Immunoprecipitation with anti-FLAG M2 affinity gel (1 µl/OD<sub>600</sub> cells) was performed for 3 h at 4°C. Bound proteins were eluted at 65°C in HU buffer and analysed by immunoblot. For Co-IP assays from chromosomally tagged strains using anti-MYC beads, total cell lysates was prepared from 100 OD<sub>600</sub> grown in YEL media. IP was performed for 3 h using 25 µl of anti-MYC agarose resin (SIGMA) followed by immunoblot assays to detect Co-IP proteins.

### Pull-down of ubiquitin conjugates under denaturing conditions

Ubiquitin conjugates were purified following protocols used for the identification of SUMO-protein conjugates (Sacher et al, 2005). Briefly, *S. pombe* cells were co-transformed with *pREP1-6HIS-MYC-Spubi4* plasmid with natMX marker (gift from Li-Lin Du) and *peno1-3MYC-sde2-3FLAG*. Total lysates from 50 OD<sub>600</sub> cells prepared under denaturing condition were used to pull-down HIS-ubiquitin

conjugates by Ni-NTA beads (Qiagen). Western blot with anti-FLAG antibody was performed to detect ubiquitin conjugates of Sde2.

### Splicing-sensitive microarray

*Schizosaccharomyces pombe* splicing-sensitive microarray design, experimental procedure and data analysis were reported earlier (Inada & Pleiss, 2010). Total RNA isolated from logarithmically growing cultures of wild-type and *Δsde2* strains was treated at 30°C and 37°C for 15 min. cDNAs from both strains were labelled with Cy3 and Cy5 dyes. Mixtures of Cy3-labelled wild-type sample and Cy5-labelled *Δsde2* sample and from dye-swapped samples were hybridized to the arrays.

### RNA isolation and RT-PCR

RNA isolation and cDNA synthesis were done as described previously (Inada & Pleiss, 2010). Briefly, five OD<sub>600</sub> cells in log phase were harvested at 30°C (untreated control) or after 15 min of heat shock at 37°C by filtration. Total RNA was isolated by hot acid phenol method using 15-ml phase lock gel heavy tubes (5 prime), followed by DNase I (Promega) treatment for 15 min at 30°C. Zymo-Spin II column (Zymo Research) was used for clean-up of RNA. cDNA synthesis from 3 μg total RNA was done using reverse transcriptase (RT) and random-hexamer primers (Invitrogen) at 42°C for 16 h. PCR and the products were analysed by agarose gel electrophoresis. Real-time quantitative PCR (qPCR) was done using SYBR green dye-based reagents (Roche). Primers used in RT-PCR assays of splicing targets are listed in Appendix Table S3.

### Accession codes

Splicing-sensitive microarray data were deposited with GEO accession number GSE97097.

**Expanded View** for this article is available online.

### Acknowledgements

We thank S. Jentsch for support to the project, A. Frost and J. Weissman for genetic screens with *S. pombe hub1* mutants, T. Ammon for help with experiment in Fig EV1D, A. Das, M. Sanjeev and S. Adusumilli for technical help, NBRP/YGRC and L.L. Du for materials and M. Sharma for comments on the manuscript. S.K.M. is supported by the Ministry of Human Resource and Development (MHRD) and Department of Science and Technology (DST), Government of India, and the Max Planck Society, Germany. P.T. and S.D. are recipients of scholarships from DST, P.A.P. from the University Grant Commission (UGC) and K.K.K. from ICMR, Government of India. The authors declare no competing financial interests.

### Author contributions

PT performed experiments on RNA splicing (Figs 1D, 3F, 4A, 5B, 6B, 7, 8B–D, and EV2B–D and EV5A, Appendix Figs S1A–E, S3C, S4B, S5, S6, S7), PAP. Sde2 processing (Figs 1B and C, 2, 3A–C, 4B–D, 6A, 8E, and EV2A, EV4, EV5B and C, Appendix Figs S1B, S2, S3A, S4B), SD N-end rule (Figs 3D and E, and EV3, Appendix Fig S3B, D and E), KKK (Fig 8A), SKM and JAP splicing microarrays (Fig 5A), all authors designed the experiments, analysed the data and prepared the manuscript, SKM wrote the article with inputs from JAP.

### Conflict of interest

The authors declare that they have no conflict of interest.

### References

- Alvarez CJ, Romfo CM, Vanhoy RW, Porter GL, Wise JA (1996) Mutational analysis of U1 function in *Schizosaccharomyces pombe*: pre-mRNAs differ in the extent and nature of their requirements for this snRNA *in vivo*. *RNA* 2: 404–418
- Ammon T, Mishra SK, Kowalska K, Popowicz GM, Holak TA, Jentsch S (2014) The conserved ubiquitin-like protein Hub1 plays a critical role in splicing in human cells. *J Mol Cell Biol* 6: 312–323
- Ast G (2004) How did alternative splicing evolve? *Nat Rev Genet* 5: 773–782
- Bachmair A, Finley D, Varshavsky A (1986) *In vivo* half-life of a protein is a function of its amino-terminal residue. *Science* 234: 179–186
- Baltz AG, Munschauer M, Schwanhäusser B, Vasile A, Murakawa Y, Schueler M, Youngs N, Penfold-Brown D, Drew K, Milek M, Wyler E, Bonneau R, Selbach M, Dieterich C, Landthaler M (2012) The mRNA-bound proteome and its global occupancy profile on protein-coding transcripts. *Mol Cell* 46: 674–690
- Bayne EH, Portoso M, Kagansky A, Kos-Braun IC, Urano T, Ekwall K, Alves F, Rappsilber J, Allshire RC (2008) Splicing factors facilitate RNAi-directed silencing in fission yeast. *Science* 322: 602–606
- Bayne EH, Bijos DA, White SA, de Lima Alves F, Rappsilber J, Allshire RC (2014) A systematic genetic screen identifies new factors influencing centromeric heterochromatin integrity in fission yeast. *Genome Biol* 15: 481
- Bessonov S, Anokhina M, Will CL, Urlaub H, Luhrmann R (2008) Isolation of an active step I spliceosome and composition of its RNP core. *Nature* 452: 846–850
- Campion Y, Neel H, Gostan T, Soret J, Bordonné R (2010) Specific splicing defects in *S. pombe* carrying a degron allele of the survival of motor neuron gene. *EMBO J* 29: 1817–1829
- Chen W, Shulha HP, Ashar-Patel A, Yan J, Green KM, Query CC, Rhind N, Weng Z, Moore MJ (2014) Endogenous U2-U5-U6 snRNA complexes in *S. pombe* are intron lariat spliceosomes. *RNA* 20: 308–320
- Doherty MF, Adelmant G, Cecchetelli AD, Marto JA, Cram EJ (2014) Proteomic analysis reveals CACN-1 is a component of the spliceosome in *Caenorhabditis elegans*. *G3: Genes—Genomes—Genetics* 4: 1555–1564
- Faesen AC, Dirac AMG, Shanmugham A, Ovaas H, Perrakis A, Sixma TK (2011) Mechanism of USP7/HAUSP activation by its C-terminal ubiquitin-like domain and allosteric regulation by GMP-synthetase. *Mol Cell* 44: 147–159
- Finley D, Bartel B, Varshavsky A (1989) The tails of ubiquitin precursors are ribosomal proteins whose fusion to ubiquitin facilitates ribosome biogenesis. *Nature* 338: 394–401
- Fujiwara H, Tanaka N, Yamashita I, Kitamura K (2013) Essential role of Ubr11, but not Ubr1, as an N-end rule ubiquitin ligase in *Schizosaccharomyces pombe*. *Yeast* 30: 1–11
- Gordon C, McGurk G, Wallace M, Hastie ND (1996) A Conditional lethal mutant in the fission yeast 26 S protease subunit mts3 is defective in metaphase to anaphase transition. *J Biol Chem* 271: 5704–5711
- Graciet E, Hu RG, Piatkov K, Rhee JH, Schwarz EM, Varshavsky A (2006) Aminoacyl-transferases and the N-end rule pathway of prokaryotic/eukaryotic specificity in a human pathogen. *Proc Natl Acad Sci USA* 103: 3078–3083
- Hochstrasser M (2009) Origin and function of ubiquitin-like proteins. *Nature* 458: 422–429

- Hooks KB, Delneri D, Griffiths-Jones S (2014) Intron evolution in *Saccharomycetaceae*. *Genome Biol Evol* 6: 2543–2556
- Huang CF, Zhu JK (2014) RNA splicing factors and RNA-directed DNA methylation. *Biology (Basel)* 3: 243–254
- Inada M, Pleiss JA (2010) Genome-wide approaches to monitor pre-mRNA splicing. *Methods Enzymol* 470: 51–75
- Janke C, Magiera MM, Rathfelder N, Taxis C, Reber S, Maekawa H, Moreno-Borchart A, Doenges G, Schwob E, Schiebel E, Knop M (2004) A versatile toolbox for PCR-based tagging of yeast genes: new fluorescent proteins, more markers and promoter substitution cassettes. *Yeast* 21: 947–962
- Jo U, Cai W, Wang J, Kwon Y, D'Andrea AD, Kim H (2016) PCNA-dependent cleavage and degradation of SDE2 regulates response to replication stress. *PLoS Genet* 12: e1006465
- Kallgren SP, Andrews S, Tadeo X, Hou H, Moresco JJ, Tu PG, Yates JR, Nagy PL, Jia S (2014) The proper splicing of RNAi factors is critical for pericentric heterochromatin assembly in fission yeast. *PLoS Genet* 10: e1004334
- Kennedy PJ, Vashisht AA, Hoe KL, Kim DU, Park HO, Hayles J, Russell P (2008) A genome-wide screen of genes involved in cadmium tolerance in *Schizosaccharomyces pombe*. *Toxicol Sci* 106: 124–139
- Kim E, Magen A, Ast G (2006) Different levels of alternative splicing among eukaryotes. *Nucleic Acids Res* 35: 125–131
- Kim DU, Hayles J, Kim D, Wood V, Park HO, Won M, Yoo HS, Duhig T, Nam M, Palmer G, Han S, Jeffery L, Baek ST, Lee H, Shim YS, Lee M, Kim L, Heo KS, Noh EJ, Lee AR et al (2010) Analysis of a genome-wide set of gene deletions in the fission yeast *Schizosaccharomyces pombe*. *Nat Biotechnol* 28: 617–623
- Kimura Y, Tanaka K (2010) Regulatory mechanisms involved in the control of ubiquitin homeostasis. *J Biochem* 147: 793–798
- Knop M, Siegers K, Pereira G, Zachariae W, Winsor B, Nasmyth K, Schiebel E (1999) Epitope tagging of yeast genes using a PCR-based strategy: more tags and improved practical routines. *Yeast* 15: 963–972
- Konarska MM, Query CC (2005) Insights into the mechanisms of splicing: more lessons from the ribosome. *Genes Dev* 19: 2255–2260
- Kouranti I, McLean JR, Feoktistova A, Liang P, Johnson AE, Roberts-Galbraith RH, Gould KL (2010) A global census of fission yeast deubiquitinating enzyme localization and interaction networks reveals distinct compartmentalization profiles and overlapping functions in endocytosis and polarity. *PLoS Biol* 8: e1000471
- Lacombe T, García-Gómez JJ, de la Cruz J, Roser D, Hurt E, Linder P, Kressler D (2009) Linear ubiquitin fusion to Rps31 and its subsequent cleavage are required for the efficient production and functional integrity of 40S ribosomal subunits. *Mol Microbiol* 72: 69–84
- Li M, Chen D, Shiloh A, Luo J, Nikolaev AY, Qin J, Gu W (2002) Deubiquitination of p53 by HAUSP is an important pathway for p53 stabilization. *Nature* 416: 648–653
- Li M, Brooks CL, Kon N, Gu W (2004) A dynamic role of HAUSP in the p53-Mdm2 pathway. *Mol Cell* 13: 879–886
- Lorenzi LE, Bah A, Wischnewski H, Shchepachev V, Sonesson C, Santagostino M, Azzalin CM (2015) Fission yeast Cactin restricts telomere transcription and elongation by controlling Rap1 levels. *EMBO J* 34: 115–129
- Mishra SK, Ammon T, Popowicz GM, Krajewski M, Nagel RJ, Ares M, Holak TA, Jentsch S (2011) Role of the ubiquitin-like protein Hub1 in splice-site usage and alternative splicing. *Nature* 474: 173–178
- Richert K, Schmidt H, Gross T, Käufer N (2002) The deubiquitinating enzyme Ubp21p of fission yeast stabilizes a mutant form of protein kinase Prp4p. *Mol Genet Genomics* 267: 88–95
- Sacher M, Pfander B, Jentsch S (2005) Identification of SUMO–protein conjugates in ubiquitin and protein degradation. *Methods Enzymol* 399: 392–404
- Sriram SM, Kim BY, Kwon YT (2011) The N-end rule pathway: emerging functions and molecular principles of substrate recognition. *Nat Rev Mol Cell Biol* 12: 735–747
- Staley JP, Woolford JL (2009) Assembly of ribosomes and spliceosomes: complex ribonucleoprotein machines. *Curr Opin Cell Biol* 21: 109–118
- Sugioka-Sugiyama R, Sugiyama T (2011) Sde2: a novel nuclear protein essential for telomeric silencing and genomic stability in *Schizosaccharomyces pombe*. *Biochem Biophys Res Commun* 406: 444–448
- Turcu FER, Ventii KH, Wilkinson KD (2009) Regulation and cellular roles of ubiquitin-specific deubiquitinating enzymes. *Annu Rev Biochem* 78: 363–397
- van der Veen AG, Ploegh HL (2012) Ubiquitin-like proteins. *Annu Rev Biochem* 81: 323–357
- Vijaykrishna N, Melangath G, Kumar R, Khandelia P, Bawa P, Varadarajan R, Vijayraghavan U (2016) The fission yeast pre-mRNA processing factor 18 (prp18\*) has intron-specific splicing functions with links to G1-S cell cycle progression. *J Biol Chem* 291: 27387–27402
- Wahl MC, Will CL, Lührmann R (2009) The Spliceosome: design principles of a dynamic RNP machine. *Cell* 136: 701–718
- Wang J, Tadeo X, Hou H, Andrews S, Moresco JJ, Yates JR, Nagy PL, Jia S (2014) Tls1 regulates splicing of shelterin components to control telomeric heterochromatin assembly and telomere length. *Nucleic Acids Res* 42: 11419–11432
- Webb CJ, Lakhe-Reddy S, Romfo CM, Wise JA (2005) Analysis of mutant phenotypes and splicing defects demonstrates functional collaboration between the large and small subunits of the essential splicing factor U2AF *in vivo*. *Mol Biol Cell* 16: 584–596
- Welchman RL, Gordon C, Mayer RJ (2005) Ubiquitin and ubiquitin-like proteins as multifunctional signals. *Nat Rev Mol Cell Biol* 6: 599–609
- Wilkinson CRM, Dittmar GAG, Ohi MD, Uetz P, Jones N, Finley D (2004) Ubiquitin-like protein Hub1 is required for pre-mRNA splicing and localization of an essential splicing factor in fission yeast. *Curr Biol* 14: 2283–2288
- Yang J, Yan R, Roy A, Xu D, Poisson J, Zhang Y (2015) The i-TASSER suite: protein structure and function prediction. *Nat Methods* 12: 7–8
- Yashiroda H, Tanaka K (2004) Hub1 is an essential ubiquitin-like protein without functioning as a typical modifier in fission yeast. *Genes Cells* 9: 1189–1197
- Zanini IMY, Sonesson C, Lorenzi LE, Azzalin CM (2017) Human Cactin interacts with DHX8 and SRRM2 to assure efficient pre-mRNA splicing and sister chromatid cohesion. *J Cell Sci* 130: 767–778
- Zhang L, Ma N, Liu Q, Ma Y (2013) Genome-wide screening for genes associated with valproic acid sensitivity in fission yeast. *PLoS One* 8: e68738